Photoplethysmography-Based Method for Automatic Detection of Premature Ventricular Contractions

Andrius Sološenko, Andrius Petrėnas, Vaidotas Marozas, *Member*, *IEEE*

***Abstract*—This work introduces a method for detection of premature ventricular contractions (PVCs) in photoplethysmogram (PPG). The method relies on 6 features, characterising PPG pulse power, and peak-to-peak intervals. A sliding window approach is applied to extract the features, which are later normalized with respect to an estimated heart rate. Artificial neural network with either linear and non-linear outputs was investigated as a feature classifier. PhysioNet databases, namely, the MIMIC II and the MIMIC, were used for training and testing, respectively. After annotating the PPGs with respect to synchronously recorded electrocardiogram, two main types of PVCs were distinguished: with and without the observable PPG pulse. The obtained sensitivity and specificity values for both considered PVC types were 92.4 / 99.9% and 93.2 / 99.9%, respectively. The achieved high classification results form a basis for a reliable PVC detection using a less obtrusive approach than the electrocardiography-based detection methods.**

***Index Terms*—PVC, PPG, MIMIC, Arrhythmia, Adaptive Filter, Extrasystoles, Artificial Neural Network (ANN)**

I. Introduction

PREMATURE ventricular contractions (PVCs) are the most commonly encountered cardiac disorder in humans. PVCs are initiated by the secondary pacemakers – the ectopic foci, located in the ventricles, therefore causing them to contract prematurely. It is well known that PVCs may occur even in healthy hearts with no significant impact on overall well-being. Accordingly, early studies have suggested that PVCs could be considered as benign in the absence of structural heart disease [1]. However, more recent studies have denied the benignity of PVCs, linking them to various health abnormalities. For example, increased frequency of PVCs has been associated with heart failure and sudden death if a heart disease was suspected [2, 3]. PVCs have also been found to be a trigger of other serious heart arrhythmias such as a ventricular fibrillation [4], and atrial fibrillation [5, 6].

Several studies have shown, e.g., [7], that PVCs have a potential to be used as a predictor of sudden cardiac death in men even without recognized heart disease. This particularly applies if frequent PVCs occur during physical exercise [2, 8], and especially during the phase of recovery [2, 9]. Since PVCs usually cause inefficiency in blood circulation, notably in cases of multiple frequent PVCs, i.e., bigeminy (every 2^{nd} beat is premature) and trigeminy (every 3^{rd} beat is premature), such condition may lead to a dizziness or a temporal loss of consciousness [10–12]. In addition, PVCs are common in patients with chronic kidney disease [13], being a consequence of electrolyte shifts (e.g., low blood potassium and calcium), resulting in electrolyte imbalance during procedures such as hemodialysis.

In most cases, PVCs have a distinctive morphology, thus are relatively easy detectable in electrocardiogram (ECG). Hence, PVC characterising properties, such as frequency and morphology, are usually evaluated using conventional Holter monitors. However, the electrodes used to record ECG are attached to the patient's chest, resulting in discomfort, limited freedom of movement, and increased feeling of unhealthiness, especially after wearing the device for several days [14].

On the contrary to Holter monitors, photoplethysmography–based devices offer a cheaper and a more convenient way for a daily life screening, since no electrodes are needed [15]. Photoplethysmography is a non-invasive technique commonly applied for monitoring of hemodynamic changes in the cardiovascular system by illuminating tissue with a certain wavelength (e.g., infrared, red, yellow, green light). In contrast to ECG electrodes, the photoplethysmographic sensors are more patient–friendly since the sensor can be attached to a finger [16], to be integrated into the ear-phones [17, 18], implemented in a forehead band [18, 19] or used as a wrist sensor [18–20]. Somehow surprisingly, only a few studies have been dedicated to PVC detection using photoplethysmography technique [16, 21, 22].

In this study, we propose a method that involves PPG pulse power-derived features in addition to the temporal features that have been explored in earlier works. An important property of the proposed method is that the temporal features are normalized according to a preceding heart rate, estimated by combining temporal preprocessing and spectral analysis. Hence, differently from the previous studies, this solution allows to detect PVCs even during the episode of bigeminy. In addition, an artifact detector was implemented in order to reduce the number of false alarms.

The paper is organized as follows: PPG waveforms together with a signal database are described in Section II, followed by a description of the proposed method in Section III. The results of PVC detection are presented in Section IV.

Preliminary results of this study were presented in a shorter conference publication [23].

Manuscript submitted on Jan 15, 2015; revised Apr 29, 2015 and May 31, 2015; accepted Sep 6, 2015. Date of publication October ??, 2015; date of current version ???? ??, 2015. *Asterisk indicates corresponding author.*

*Andrius Sološenko is with the Biomedical Engineering Institute, Kaunas University of Technology, Kaunas, Lithuania (e-mail: andrius.solosenko@ktu.lt).

Andrius Petrėnas is with the Biomedical Engineering Institute, Kaunas University of Technology, Kaunas, Lithuania.

Vaidotas Marozas is with the Dept. of Electronics Engineering and Biomedical Engineering Institute, Kaunas University of Technology, Kaunas, Lithuania.

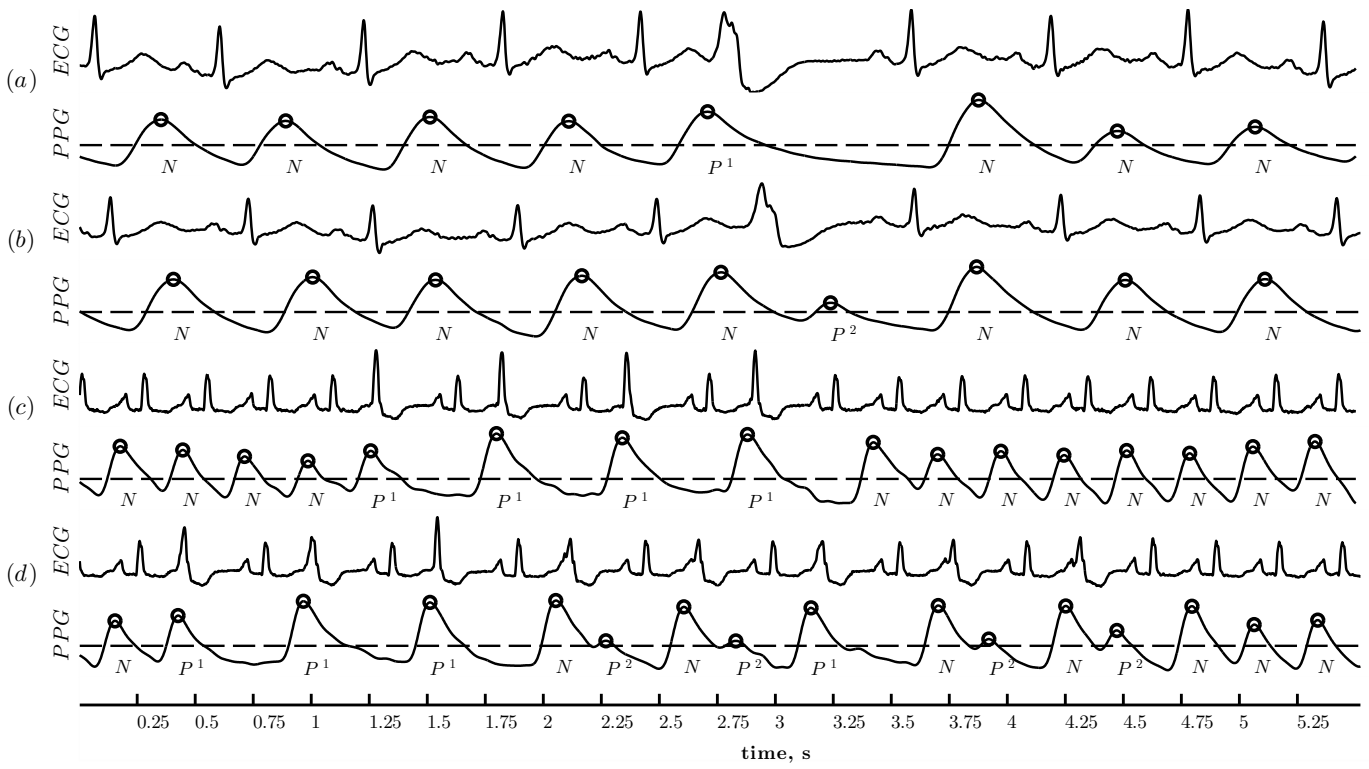

Fig. 1. Examples of PVC pulse types in PPG together with reference ECG: (a) PPG pulses during normal sinus rhythm (labelled as N) with a single PVC that is not followed by any observable pulse (labelled as P^1), (b) a single PVC characterized by a small pulse amplitude (labelled as P^2), (c), consecutive type P^1 pulses (bigeminy), (d) bigeminy with both PVC pulse types. In this particular example, ECGs and PPGs were preprocessed with zero-phase band-pass filters having cut-off frequencies of 0.05-150 Hz and 0.4-15 Hz, respectively

II. PPG WAVEFORMS AND DATASET

A. Waveforms

It is well-known that the alternating part of the PPG is proportional to the peripheral blood volume changes [24]. Premature contractions result in a reduced ventricular filling, diminishing the peripheral pulse amplitude [25]. Therefore, the PPG pulses during PVC may become hardly recognizable (Fig. 1 (a)), or may still have a sufficient amplitude for peak detection (Fig. 1 (b)). These two types of premature pulses in the PPG are denoted as P^1 and P^2, respectively.

B. Dataset

The algorithm was developed on 18 PPGs (training set), sampled at 125 Hz, which were taken from the PhysioNet MIMIC II database [26, 27]. Twenty-five 1-2 h PPGs, sampled at 250 Hz (the MIMIC database [28]), and 1 signal sampled at 250 Hz of 100 min (recorded in Kaunas Biomedical Engineering Institute, labelled as BMEI) were used for testing. To reduce the errors that may occur during feature extraction, all signals were resampled to 500 Hz.

PVCs in the PPG were annotated with respect to a synchronously recorded reference ECG. At first, PVCs in the ECG were detected by using an automated RR interval detection algorithm [29]. Then, RR intervals were used for manual evaluation of ECG morphology to ensure that the particular beat is PVC. Finally, PVC-related PPG pulses were labelled as P^1 or P^2 according to the previously described procedure. The remaining PPG pulses were assigned to normal N.

TABLE I
TEST PPGS OBTAINED FROM THE MIMIC DATABASE (NO. 1-25) AND RECORDED IN KTU BME INSTITUTE (NO. 26)

No.	Signal name	#P^1	#P^2	No.	Signal name	#P^1	#P^2
1	039m	0	0	14	404m	0	268
2	041m	0	0	15	408m	9	2
3	055m	1	0	16	439m	12	3
4	211m	0	0	17	442m	1288	366
5	212m	159	30	18	444m	7	10
6	218m	0	0	19	449m	7	2
7	221m	11	0	20	466m	3	4
8	224m	0	0	21	471m	1	0
9	225m	0	11	22	474m	2	4
10	230m	0	4	23	482m	48	88
11	237m	40	14	24	484m	69	20
12	252m	0	0	25	485m	754	16
13	253m	0	0	26	BMEI	25	2
	Total:	211	59		Total:	2225	785

Since the signals in both databases (MIMIC and MIMIC II) contain severe signal corruptions or various pathologies, several of them were excluded from the study. The criteria for discarding the signals was the absence of usable information in either ECG or PPG, therefore resulting in difficulties to correctly annotate the signals. The list of the test signals is presented in Table I.

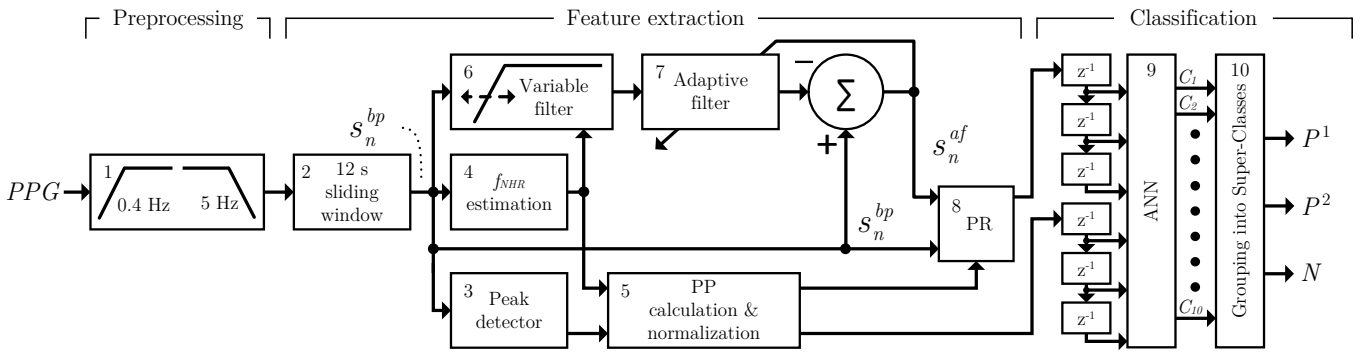

Fig. 2. Block diagram of the proposed method. Here f_{NHR} is a normal heart rate, PP is a peak-to-peak interval, PR is a power ratio, ANN is an artificial neural network, s^{bp} is a preprocessed PPG, s^{af} is a PPG with higher frequency components removed

III. Method

The proposed method for PVC detection and classification exploits temporal (peak-to-peak intervals, PPs) and power-derived (the power ratios, PRs) features, obtained for each PPG pulse. The method is composed of 3 major parts: PPG preprocessing, feature extraction, and classification (see Fig. 2).

A. Preprocessing and feature extraction

To minimize high frequency noise and baseline wandering, PPGs are preprocessed by using low-pass and high-pass finite impulse response (FIR) filters with 5 Hz and 0.4 Hz cut-off frequencies, respectively, thus resulting in a signal s^{bp} (Fig. 2 block 1). These cut-off frequencies correspond to approximal maximal and minimal physiological heart rates. A 12 s sliding analysis window with 50% overlap is used for feature extraction (Fig. 2 block 2). Positive peaks of the preprocessed PPG are detected by using threshold crossing technique (Fig. 2 block 3). Then, series of operations are applied (Fig. 2 block 4) for estimation of a normal heart rate (f_{NHR}) (see Fig. 3).

Fig. 3. Block diagram of the normal heart rate estimator. Here s^{bp} is a 12 s segment of the preprocessed PPG

When estimating f_{NHR}, it is crucial to reduce the influence of impulse noise, i.e., noise of higher amplitude than PPG, which may be falsely associated to f_{NHR} during spectral analysis. First, PPG is clipped in the empirically determined range of $\pm 0.7 std$ of the preprocessed PPG, and smoothed by applying a moving average filter. Then, the 1^{st} derivative of the resulting PPG is calculated. The 1^{st} derivative acts as a high pass filter that emphasizes higher frequency components of the PPG. In addition, the 1^{st} derivative is particularly useful when PPG segments contain bigeminy episodes, which result in nearly 2 times lower PPG pulse rate compared to a normal rhythm (see Fig. 1 (c)). Next, f_{NHR} is estimated by taking the frequency at the maximal amplitude of the power spectral density (PSD) function. Finally, outliers are removed by filtering the array of f_{NHR} using a 3^{rd} order median filter.

Normally, heart rate is inversely related to PP intervals. However, for a specific PVC type (cf. Fig. 1 (a) and (c)), the length of PP can be approximately twice the length of the interval between the subsequent PPG pulses occurring during normal rhythm. Therefore, in order to make PPs heart rate independent, PP-related features are normalized before applying them to classifier. One way to normalize PP intervals is to calculate the ratio of the current and the mean values of the intervals [22]. However, the former normalization principle is sensitive to erroneously detected PP value, i.e., during bigeminy or artifacts. Hence, PP-related features are normalized (Fig. 2 block 5) with respect to f_{NHR}:

$$PP_j = \frac{\left(\, p_{\,j} - p_{\,j-1} \, \right) f_{NHR}}{f_s}, \tag{1}$$

where j is a PP number, p_j is an array of index value of detected positive peaks, f_s is a sampling frequency (Hz), and f_{NHR} is a normal heart rate (Hz). Normalized PP intervals are close to 1 during normal heart rhythm, whereas take either lower or higher values during PVCs.

The second high-pass FIR filter is characterized by a variable cut-off frequency (Fig. 2 block 6), and is employed for the purpose to extract higher frequency components of PPG (from f_{NHR} to 5 Hz). The cut-off frequency is adjusted according to the current value of f_{NHR}. Then, the resulting signal is used as a reference input to a pre-whitened recursive least squares (RLS) adaptive filter (Fig. 2 block 7) [30]. The order and the forgetting factor of RLS filter were set to 10 and 0.999, respectively. Given that PPG pulses during PVCs are composed of lower frequency components compared to normal rhythm, subtraction of higher frequencies produce a signal s^{af}, which consists solely of premature pulses. Therefore, the amplitude of PVCs is not affected, while the PPG pulses are suppressed considerably during a normal heart rate (Fig. 4 (c)).

The power ratios (PRs) are computed in segments between two adjacent PPG pulses by involving both preprocessed PPG s^{bp} and the signal s^{af}:

$$PR_k = \frac{\sum\limits_{n=1}^{N} \left(\, s_n^{af} - \overline{s^{af}} \, \right)^2}{\sum\limits_{n=1}^{N} \left(\, s_n^{bp} - \overline{s^{bp}} \, \right)^2}, \tag{2}$$

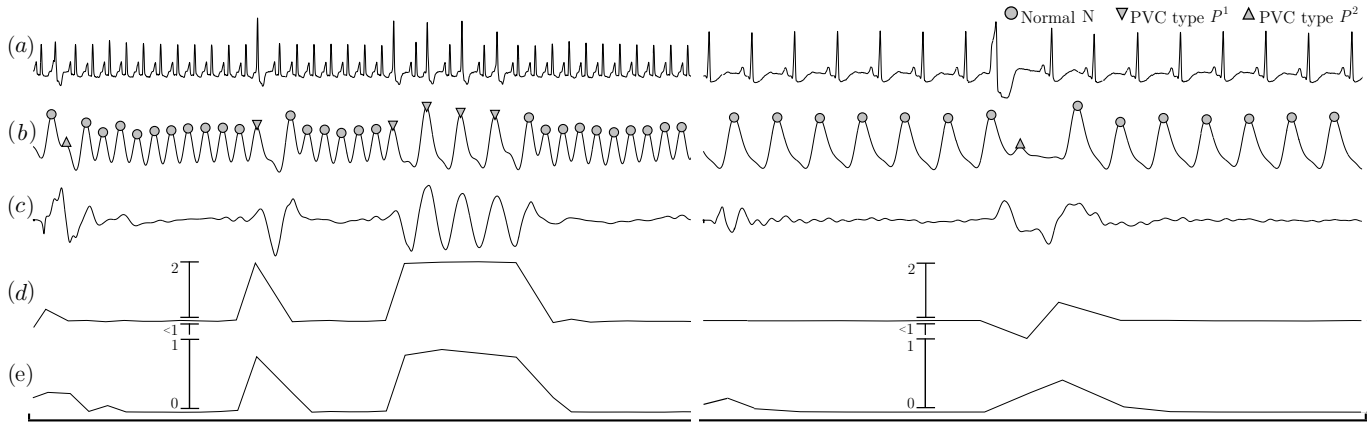

Fig. 4. Example of detected PVCs in the PPG: (a) reference ECG, (b) preprocessed PPG with PVCs (s^{bp}), (c) output of the adaptive filter (s^{af}), (d) normalized peak-to-peak intervals (PPs), and (e) power ratios (PRs). The vertical lines in (d) and (e) denote the ranges of the normalized PP and PR values, respectively.

where k is a segment number, N is a segment length (total samples in PP interval), $\overline{s^{af}}$ is a mean amplitude of samples in s^{af}, and $\overline{s^{bp}}$ is a mean amplitude of samples in s^{bp}. Since PPG amplitude is markedly suppressed in normal beats, the power ratios PR take lower values than in PVCs.

B. Classification

Feed-forward artificial neural network (ANN) with either linear or non-linear outputs was investigated for classification of individual PPG pulses (Fig. 5).

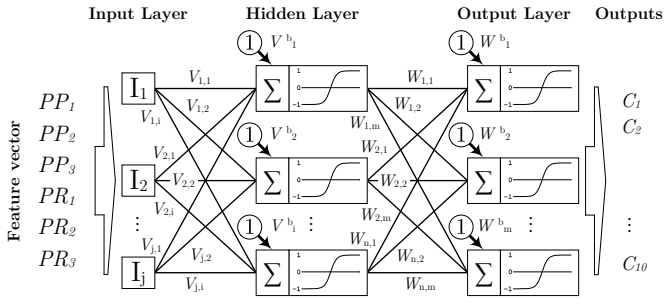

Fig. 5. Block diagram of the ANN-based PPG pulse classifier. Here I stands for ANN inputs, V are input and hidden layers connecting weights, V^b are biases of hidden neurons, W are hidden and output layers connecting weights, W^b are biases of the neurons in the output layer, and C are the outputs of the ANN (classes)

Since each individual PPG pulse is described by 3 intervals (preceding, current and subsequent), various interval combinations are feasible, therefore it is reasonable to distinguish many classes (i.e., 10, see Table II) in order to reduce a misclassification rate. These 10 classes (Fig. 1 block 9) are further grouped into 3 super-classes, denoted by P^1, P^2 and N, respectively (Fig. 1 block 10). The full list of classes and super-classes is presented in Table II.

The number of neurons in a hidden layer of ANN was chosen empirically, and was set to 40. A back-propagation method was used for training [31]. To cope with the overfitting, a small random noise was added to each of the input [32]. Both ANN and back-propagation learning method were implemented in Matlab environment.

TABLE II
PPG PULSE CLASSIFICATION INTO (a) 10 CLASSES AND (b) 3 SUPER-CLASSES

(a)	C_1 ($Normal$)	C_2 ($Normal$ before P^1)	C_3 ($Normal$ after P^1)	C_4 ($Normal$ before P^2)	C_5 ($Normal$ after P^2)	C_6 ($Bigeminy\ start$)	C_7 ($Bigeminy$)	C_8 ($Bigeminy\ end$)	C_9 ($Single\ P^1$)	C_{10} ($Single\ P^2$)
(b)	N					P^1				P^2

C. Artifact detection

Motion and tissue deformation induced artifacts is a crucial issue hindering the development of arrhythmia detectors that are based on the PPG. To reduce the number of false alarms due to falsely detected pulses, an artifact detector is implemented.

The process of artifact detection is illustrated in Fig. 6. In the analysis window, artifacts are flagged with respect to the ratio, obtained by dividing the clipped PPG by the preprocessed (Fig. 6 (a)). Since the clipped PPG has lower amplitude, the ratio approaches to 0 when artifacts occur. PPG is flagged as an artifact whenever the empirically determined threshold exceeds 0.3. In addition, 4 pulses before and after the artifact are excluded from classification.

D. Performance evaluation

The performance of the method was evaluated in terms of sensitivity (Se), specificity (Sp) and accuracy (Acc). Due to the a considerable difference in a number of normal pulses and PVCs, the Matthews correlation coefficient was employed as an additional performance measure (MCC) [33].

The method was tested by using ANN with either linear and non-linear outputs. The full feature set (3 PP and 3 PR) was applied for training the ANN. In addition, the performance was also tested with a reduced feature set, consisting of just

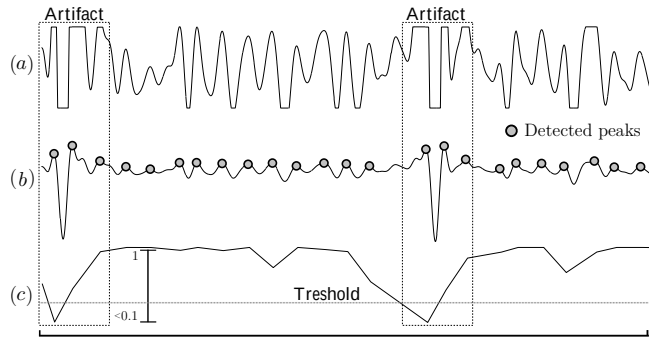

Fig. 6. Example of artifact detection in the PPG: (a) the clipped PPG, (b) the preprocessed PPG, and (c) the ratio of the signals in (a) and (b). Vertical line denotes the ranges of ratio values

3 PP inputs. Since, the weights in the ANN are initialized randomly, the training process has been repeated 3 times, and then the averaged performance values were taken as the overall performance measure.

It should be noted that the initial testing was carried out without involving artifact detection. Then, both the best performing, and the most computationally efficient (with PP features, linear outputs, and the blocks 6, 7 and 8 excluded in Fig. 2) configurations were used for a repeated testing but with the artifact detector involved.

IV. Results

The results are presented in Tables III–VI. Table III shows that the performance of ANN does not depend on the type of neurons in the output layer, although slightly better results are obtained when an ANN with the linear outputs is used. On the other hand, ANN that employs only PP feature set is associated with a higher accuracy when non-linear outputs are used (Table IV).

The ANN with linear outputs and full feature set was further reinvestigated but with the artifact detector included. The inclusion of the artifact detector allowed to reduce a number of false positives by approximately 60%. Thus, the Sp for PVC types P^1 and P^2 increased from 99.6 / 99.8% to 99.9 / 99.9%, respectively. However, the inclusion of the artifact detector resulted in a slight decrease in Se from 94.2 / 93.1% to 93.2 / 92.4%, respectively (Table V). The decrease in sensitivity can be explained by the fact that some of premature pulses have similar morphology to artifacts, and therefore have been removed from further analysis.

The most computationally efficient configuration is associated with a slightly worse performance compared to the best performing configuration (see Tables V and VI). By combining this configuration with the artifact detector, a number of false positives decreased by approximately 63% compared to that without the artifact detector. Moreover, Sp for the P^1 PVC type increased from 99.6% to 99.9%. In contrast, Sp for P^2 PVC type remained unchanged. According to previous explanation, a slight decrease in Se is observed for both PVC pulse types, i.e., from 90.5 / 84.0% to 89.5 / 83.2% for P^1 and P^2, respectively.

TABLE III
The classification results obtained using both PP and PR features as an input to ANN: (a) performance measures, (b) confusion matrices

		Linear output ANN			**Non-linear output ANN**		
	Class ⇒	N	P^1	P^2	N	P^1	P^2
(a)	$Se, \%$	99.4	94.2	93.1	99.3	93.2	91.6
	$Sp, \%$	94.2	99.6	99.8	93.1	99.5	99.8
	$Acc, \%$	99.3	99.5	99.8	99.3	99.5	99.8
	$MCC, \%$	78.3	79.3	75.2	78.0	77.5	75.2
	Class ⇒	N	P^1	P^2	N	P^1	P^2
(b)	N	255002	133	57	254867	156	70
	P^1	1122	2295	1	1236	2271	1
	P^2	496	8	786	468	9	773

TABLE IV
The classification results obtained using solely PP-based features: (a) performance measures, (b) confusion matrices

		Linear output ANN			**Non-linear output ANN**		
	Class ⇒	N	P^1	P^2	N	P^1	P^2
(a)	$Se, \%$	99.3	90.5	84.0	99.0	91.2	91.0
	$Sp, \%$	89.1	99.6	99.8	92.6	99.4	99.7
	$Acc, \%$	99.2	99.5	99.7	99.0	99.3	99.7
	$MCC, \%$	74.4	77.1	66.8	71.7	73.5	66.5
	Class ⇒	N	P^1	P^2	N	P^1	P^2
(b)	N	255069	222	134	253302	186	53
	P^1	1134	2205	1	1499	2237	0
	P^2	610	9	709	768	13	746

V. Discussion

The goal of this work was to develop a method for detection of premature ventricular contractions by relying solely on photoplethysmography signal analysis. Our first attempt to detect premature contractions by using PPG was presented in an earlier study [34]. Besides that the pilot study was performed on the basis of just 9 PPG signals, the previous algorithm, in contrast to the proposed, had limited capabilities of detecting successive premature pulses such as bigeminy.

In contrast to ECG, the PPG can be acquired in a single spot of the body, let alone the fact that no adhesive electrodes are required. Considering these points, PPG-based arrhythmia detection is an attractive solution for both short-term screening and long-term arrhythmia monitoring when unobtrusiveness for the user is of special importance.

The proposed PVC detector, thanks to the blocks of adaptive feature extraction and artifact detection, allowed to achieve better performance than that obtained by Gil et al. [22]. Even though, Gil et al. excluded PVCs that had occurred within 5 previous or 20 subsequent beats, our method was more accurate (99.8 vs. 99.3%).

The study revealed that the main challenge is to distinguish PVCs from artifacts, since the distorted PPG pulse can be

TABLE V
THE CLASSIFICATION RESULTS OBTAINED USING LINEAR OUTPUT ANN CLASSIFIER, BOTH PP AND PR FEATURES AND ARTIFACT DETECTOR: (a) PERFORMANCE MEASURES, (b) CONFUSION MATRICES

	Class ⇒	N	P^1	P^2
(a)	$Se, \%$	99.8	93.2	92.4
	$Sp, \%$	93.3	99.9	99.9
	$Acc, \%$	99.7	99.8	99.8
	$MCC, \%$	87.7	91.3	78.7
	Class ⇒	N	P^1	P^2
(b)	N	255891	158	63
	P^1	262	2270	1
	P^2	373	8	780

TABLE VI
THE CLASSIFICATION RESULTS OBTAINED USING LINEAR OUTPUT ANN, PP FEATURES AND ARTIFACT DETECTOR: (a) PERFORMANCE MEASURES, (b) CONFUSION MATRICES

	Class ⇒	N	P^1	P^2
(a)	$Se, \%$	99.7	89.5	83.2
	$Sp, \%$	88.2	99.9	99.8
	$Acc, \%$	99.5	99.8	99.7
	$MCC, \%$	81.9	87.5	68.3
	Class ⇒	N	P^1	P^2
(a)	N	254696	246	137
	P^1	362	2181	1
	P^2	523	9	683

erroneously assigned to a class of premature beat. Thus is, high amplitude artifacts may usually distort a group of nearby pulses and introduce residual distortions in a shape of further pulses. Nevertheless, even the simplified configuration of the algorithm showed sufficient performance to detect PVCs in artifact-distorted PPGs (see Table IV (a)). Therefore, the simplified (computationally efficient) configuration can be considered for the implementation in a mobile device.

Although the algorithm shows nearly perfect specificity (99.9%), the specificity can be further improved by computing PRs in several discrete ranges of each PP, rather than obtaining PRs in the entire PP interval. Additional improvement in specificity may be achieved by upgrading an artifact detector, since the current artifact detector is effective only in cases when artifacts have higher amplitude than a normal PPG pulse.

In this study, high-pass and low-pass FIR filters were used to pre-process the PPG. However, more advanced signal processing techniques can be employed either to eliminate PPG distortions, such as baseline wandering [35, 36], or to assess PPG quality [37, 38]. Initial tests showed that a single-layer perceptron classifier does not converge during training, owing to the fact that the PPG features used in the present study are not linearly separable. Hence, a multi-layer perceptron (i.e., ANN) was chosen due to its universal characteristics and ability to approximate linear and non-linear functions. In addition, the performance of PPG pulse classification largely depends on an estimated normal heart rate (parameter f_{NHR}) which influences the normalization process.

The presented study has several limitations. Firstly, the signals have not been annotated by the medical experts. Secondly, the method has not been tested on the signals recorded during active motion, such as walking and jogging. Finally, for some rare PVC types (e.g., interpolated PVCs) [39], PVCs can not be detected by the algorithm because PPG is not enough sensitive to hemodynamic changes during such cardiac events.

VI. CONCLUSIONS AND SIGNIFICANCE OF THE WORK

A photoplethysmography-based method for detection of premature ventricular contractions has been developed. Considering its high performance, the proposed PVC detector is expected to have both a non-clinical (e.g., sleep monitoring) and a clinical (e.g., in hemodialysis procedures) relevance when moderate physical activity is involved.

APPENDIX

The appendix briefly describes an online implementation of the proposed method. The online version of the method was implemented as the application for the use in Android operating system. The most computationally efficient configuration of the algorithm (i.e., PP features, linear ANN outputs, and the blocks 6, 7 and 8 excluded in Fig. 2) was selected for the implementation. The PPG is transmitted to the smartphone via Bluetooth connection.

Figure 7 shows a screenshot of the application running on the smartphone. PPG segment with correctly detected PVCs during the episode of bigeminy is shown in a chart on the top of the application window. The bottom chart shows the normalized peak-to-peak intervals. The sliding panel on the right side provides an important information about the number of detected PVCs and the PVC burden, determined by a percentage of PVC-related beats compared to a total number of beats.

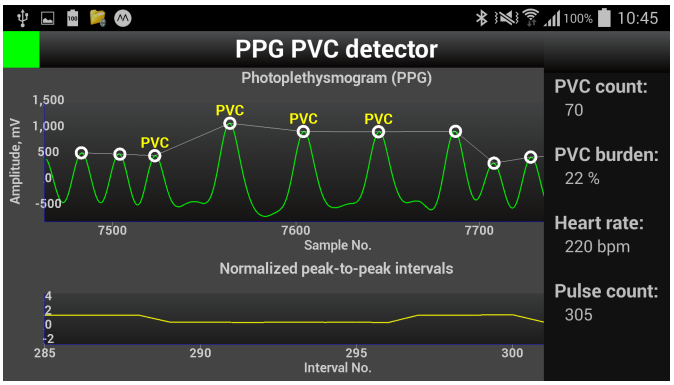

Fig. 7. Screenshot of the Android application with the implemented PVC detection algorithm. An application window shows detected PVCs during bigeminy episode, and other heart rhythm related parameters. Note that this particular signal is characterized by a very high heart rhythm (220 bpm) outside the episode of multiple PVCs

ACKNOWLEDGEMENT

This work was partially supported by CARRE (No. 611140) project, funded by the European Commission Framework Program 7, and by the Research Council of Lithuania (Agreement No. MIP-15391).

REFERENCES

[1] H. L. Kennedy, J. A. Whitlock, and M. K. Sprague, "Long-term follow-up of asymptomatic healthy subjects with frequent and complex ventricular ectopy," *New England Journal of Medicine*, vol. 312, no. 4, pp. 193–197, 1985.

[2] G. A. Ng, "Treating patients with ventricular ectopic beats," *Heart*, vol. 92, no. 11, pp. 1707–1712, 2006.

[3] G. Ephrem, M. Levine, P. Friedmann, and P. Schweitzer, "The prognostic significance of frequency and morphology of premature ventricular complexes during ambulatory Holter monitoring," *Annals of Noninvasive Electrocardiology*, vol. 18, no. 2, pp. 118–125, 2013.

[4] F. Santoro, L. d. Biase, P. Hranitzky, J. E. Sanchez, P. Santangeli, A. P. Perini, J. D. Burkhardt, and A. Natale, "Ventricular fibrillation triggered by PVCs from papillary muscles: Clinical features and ablation," *Journal of Cardiovascular Electrophysiology*, vol. 25, no. 11, pp. 1158–1164, 2014.

[5] H. Watanabe, N. Tanabe, and Y. Makiyama, "ST-segment abnormalities and premature complexes are predictors of new-onset atrial fibrillation: The Niigata preventive medicine study," *American Heart Journal*, vol. 152, no. 4, pp. 731–735, 2006.

[6] S. K. Agarwal, G. Heiss, P. M. Rautaharju, and et al., "Premature ventricular complexes and the risk of incident stroke: the Atherosclerosis Risk In Communities (ARIC) Study." *Stroke; a journal of cerebral circulation*, vol. 41, pp. 588–93, Apr 2010.

[7] H. Hirose, S. Ishikawa, T. Gotoh, T. Kabutoya, K. Kayaba, and E. Kajii, "Cardiac mortality of premature ventricular complexes in healthy people in Japan," *Journal of Cardiology*, vol. 56, no. 1, pp. 23 – 26, 2010.

[8] X. Jouven, M. Zureik, and M. Desnos, "Long-term outcome in asymptomatic men with exercise-induced premature ventricular depolarizations," *New England Journal of Medicine*, vol. 343, no. 12, pp. 826–833, 2000.

[9] J. P. Frolkis, C. E. Pothier, and E. H. Blackstone, "Frequent ventricular ectopy after exercise as a predictor of death," *New England Journal of Medicine*, vol. 348, no. 9, pp. 781–790, 2003.

[10] B. Zaret, L. Cohen, and M. Moser, *Yale University School of Medicine Heart Book*. William Morrow and Co., 1992.

[11] M. J. Reed and A. Gray, "Collapse query cause: the management of adult syncope in the emergency department," *Emerg Med J*, vol. 23, no. 8, pp. 589–594, Aug 2006.

[12] A. Garcia-Touchard, V. K. Somers, T. Kara, J. Nykodym, A. Shamsuzzaman, P. Lanfranchi, and M. J. Ackerman, "Ventricular ectopy during rem sleep: implications for nocturnal sudden cardiac death," *Nat Clin Pract Cardiovasc Med*, vol. 4, no. 5, pp. 284–288, May 2007.

[13] P. S. P. M. Khaled Shamseddin, "Sudden cardiac death in chronic kidney disease: epidemiology and prevention," *Nature Reviews Nephrology*, no. 3, pp. 145–154, 2011.

[14] S. Z. Rosero, V. Kutyifa, B. Olshansky, and W. Zareba, "Ambulatory ecg monitoring in atrial fibrillation management," *Progress in Cardiovascular Diseases*, vol. 52, no. 2, pp. 143–152, 2013.

[15] J. Allen, "Photoplethysmography and its application in clinical physiological measurement," *Physiol. Meas.*, vol. 28, no. 3, pp. 1–39, 2007.

[16] T. Suzuki, K.-I. Kameyama, and T. Tamura, "Development of the irregular pulse detection method in daily life using wearable photoplethysmographic sensor," in *Engineering in Medicine and Biology Society, 2009. EMBC 2009. Annual International Conference of the IEEE*, Sept 2009, pp. 6080–6083.

[17] L. Wang, B. Lo, and G.-Z. Yang, "Multichannel reflective ppg earpiece sensor with passive motion cancellation," *Biomedical Circuits and Systems, IEEE Transactions on*, vol. 1, no. 4, pp. 235–241, Dec 2007.

[18] T. Tamura, Y. Maeda, M. Sekine, and M. Yoshida, "Wearable photoplethysmographic sensors – past and present," *Electronics*, vol. 3, no. 2, pp. 282–302, 2014.

[19] K. Li and S. Warren, "A wireless reflectance pulse oximeter with digital baseline control for unfiltered photoplethysmograms," *Biomedical Circuits and Systems, IEEE Transactions on*, vol. 6, no. 3, pp. 269–278, June 2012.

[20] R. Haahr, S. Duun, M. Toft, B. Belhage, J. Larsen, K. Birkelund, and E. Thomsen, "An electronic patch for wearable health monitoring by reflectance pulse oximetry," *Biomedical Circuits and Systems, IEEE Transactions on*, vol. 6, no. 1, pp. 45–53, Feb 2012.

[21] K. H. Shelley, "Photoplethysmography: beyond the calculation of arterial oxygen saturation and heart rate," *Anesth. Analg.*, vol. 105, no. 6 Suppl, pp. S31–36, Dec 2007.

[22] E. Gil, P. Laguna, J. Martinez, O. Barquero-Perez, A. Garcia-Alberola, and L. Sornmo, "Heart rate turbulence analysis based on photoplethysmography," *Biomedical Engineering, IEEE Transactions on*, vol. 60, no. 11, pp. 3149–3155, Nov 2013.

[23] A. Solosenko and V. Marozas, "Automatic premature ventricular contraction detection in photoplethysmographic signals," in *2014 IEEE BioCAS Proceedings*, ser. IEEE Proceedings, 2014, pp. 49–52.

[24] E. Peper, R. Harvey, I.-M. Lin, H. Tylova, and D. Moss, "Is there more to blood volume pulse than heart rate variability respiratory sinus arrhythmia, and cardiorespiratory synchrony?" *Biofeedback*, vol. 35, no. 2, pp. 54–61, 2007.

[25] D. Zheng, J. Allen, and A. Murray, "Determination of aortic valve opening time and left ventricular peak filling rate from the peripheral pulse amplitude in patients with ectopic beats," *Physiological Measurement*, vol. 29, no. 12, pp. 1411–1419, 2008.

[26] A. L. Goldberger, L. A. N. Amaral, L. Glass, J. M. Hausdorff, P. C. Ivanov, R. G. Mark, J. E. Mietus, G. B. Moody, C.-K. Peng, and H. E. Stanley, "Physiobank, physiotoolkit, and physionet: Components of a new research resource for complex physiologic signals," *Circulation*, vol. 101, no. 23, pp. 215–220, 2000.

[27] M. Saeed, M. Villarroel, A. T. Reisner, G. Clifford, L.-W. Lehman, G. Moody, T. Heldt, T. H. Kyaw, B. Moody, and R. G. Mark, "Multiparameter intelligent monitoring in intensive care ii (mimic-ii): A public-access intensive care unit database," *Critical Care Medicine*, vol. 39, pp. 952–960, May 2011.

[28] G. Moody and R. Mark, "A database to support development and evaluation of intelligent intensive care monitoring," in *Computers in Cardiology, 1996*, Sept 1996, pp. 657–660.

[29] D. S. Benitez, P. Gaydecki, A. Zaidi, and A. P. Fitzpatrick, "The use of the hilbert transform in ecg signal analysis." *Comp. in Bio. and Med.*, vol. 31, no. 5, pp. 399–406, 2001.

[30] S. Douglas, "Numerically-robust o(n^2) RLS algorithms using least-squares prewhitening," in *Acoustics, Speech, and Signal Processing, 2000. ICASSP '00. Proceedings. 2000 IEEE International Conference on*, vol. 1, 2000, pp. 412–415 vol.1.

[31] T. Vogl, J. Mangis, A. Rigler, W. Zink, and D. Alkon, "Accelerating the convergence of the back-propagation method," *Biological Cybernetics*, vol. 59, no. 4-5, pp. 257–263, 1988.

[32] Piotrowski, A. P., Napiorkowski, and J. J., "A comparison of methods to avoid overfitting in neural networks training in the case of catchment runoff modelling," *Journal of Hydrology*, vol. 476, pp. 97 – 111, 2013.

[33] J. Gorodkin, "Comparing two k-category assignments by a k-category correlation coefficient," *Computational Biology and Chemistry*, vol. 28, no. 5-6, pp. 367–374, 2004.

[34] A. Solosenko and V. Marozas, "Automatic extrasystole detection using photoplethysmographic signals," in *XIII Mediterranean Conference on Medical and Biological Engineering and Computing 2013*, ser. IFMBE Proceedings, 2013, vol. 41, pp. 985–988.

[35] P. Laguna, R. Jane, and P. Caminal, "Adaptive filtering of ECG baseline wander," in *Engineering in Medicine and Biology Society, 1992 14th Annual International Conference of the IEEE*, vol. 2, Oct 1992, pp. 508–509.

[36] H. Wang, X. Wang, J. Deller, and J. Fu, "Shape-preserving preprocessing for human pulse signals based on adaptive parameter determination," *Biomedical Circuits and Systems, IEEE Transactions on*, vol. 8, no. 4, pp. 594–604, Aug 2014.

[37] J. Patterson and G.-Z. Yang, "Ratiometric artifact reduction in low power reflective photoplethysmography," *Biomedical Circuits and Systems, IEEE Transactions on*, vol. 5, no. 4, pp. 330–338, Aug 2011.

[38] K. Li, S. Warren, and B. Natarajan, "Onboard tagging for real-time quality assessment of photoplethysmograms acquired by a wireless reflectance pulse oximeter," *Biomedical Circuits and Systems, IEEE Transactions on*, vol. 6, no. 1, pp. 54–63, Feb 2012.

[39] J. Reilly and H. Antoni, *Electrical Stimulation and Electropathology*. Cambridge University Press, 1992.

Andrius Solosenko was born in 1988. He received the BSc. degree in electronics engineering and MSc. degree in biomedical engineering from Kaunas University of Technology, Kaunas, Lithuania in 2011 and 2013, respectively. He is PhD student of electronics engineering since 2013 in Kaunas University of Technology. His current areas of research are digital signal processing algorithms for cardiac event detection in optical signals and development of medical mobile applications.

Andrius Petrėnas received the B.Sc. degree in electronics engineering and the M.Sc. degree in biomedical engineering from Kaunas University of Technology, Kaunas, Lithuania, in 2009 and 2011, respectively. He is currently with the Biomedical Engineering Institute at Kaunas University of Technology where he is working toward the Ph.D. degree. His research interests are mainly concentrated on signal processing algorithms for long-term monitoring of paroxysmal atrial fibrillation, with particular interest in detection of brief arrhythmia episodes.

Vaidotas Marozas received the BSc., MSc., and PhD. degrees in electrical engineering from Kaunas University of Technology (KTU), Kaunas, Lithuania, in 1993, 1995, and 2000 rectively. He was a visiting PhD student for several time periods during 1998 – 2000 in the Signal Processing Group, Department of Electroscience, Lund University, Lund, Sweden. Since 2001, he has been with Department of Electronics, Faculty of Electrical and Electronics Engineering, KTU, where he is currently an Associate Professor. He is also affiliated with Biomedical Engineering Institute, KTU, where he is a Research Scientist. His research interests fall in the area of signal processing and embedded systems for biomedical applications: detection and characterization of cardiac arrhythmias in ECG, PPG and IPG signals, application of electroconductive textiles for physiological signals monitoring, and real-time signal processing algorithms for embedded systems.